Chemistry of the Diazeniumdiolates. 2. Kinetics and Mechanism of Dissociation to Nitric Oxide in Aqueous Solution

Keith M. Davies,*,† David A. Wink,‡ Joseph E. Saavedra,§ and Larry K. Keefer‡

Contribution from the Department of Chemistry, George Mason University, Fairfax, Virginia 22030, Chemistry Section, Laboratory of Comparative Carcinogenesis, National Cancer Institute at Frederick, Frederick, Maryland 21702, and the Intramural Research Support Program, SAIC Frederick, National Cancer Institute at Frederick, Frederick, Maryland 21702

Received August 4, 2000. Revised Manuscript Received November 22, 2000

Abstract: Diazeniumdiolate ions of structure $R_2N[N(O)NO]^-$ (**1**) are of pharmacological interest because they spontaneously generate the natural bioregulatory species, nitric oxide (NO), when dissolved in aqueous media. Here we report the kinetic details for four representative reactivity patterns: (a) straightforward dissociation of the otherwise unfunctionalized diethylamine derivative **2** (anion **1**, where R = Et) to diethylamine and NO; (b) results for the zwitterionic piperazin-1-yl analogue **4**, for which the protonation state of the neighboring basic amine site is an important determinant of dissociation rate; (c) data for **5**, a diazeniumdiolate derived from the polyamine spermine, whose complex rate equation can include terms for a variety of medium effects; and (d) the outcome for triamine **6** ($R = CH_2CH_2NH_3^+$), the most stable structure **1** ion identified to date. All of these dissociations are acid-catalyzed, with equilibrium protonation of the substrate preceding release of NO. Specific rate constants and pK_a values for **2**−**6** have been determined from pH/rate profiles. Additionally, a hypsochromic shift (from ∼250 to ∼230 nm) was observed on acidifying these ions, allowing determination of a separate pK_a for each substrate. For **6**, the pK_a value obtained kinetically was 2−3 pK_a units higher than the value obtained from the spectral shift. Comparison of the ultraviolet spectra for **6** at various pH values with those for O- and N-alkylated diazeniumdiolates suggests that protonation at the R_2N nitrogen initiates dissociation to NO at physiological pH, with a second protonation (at oxygen) accounting for both the spectral change and the enhanced dissociation rate at pH <4. Our results help to explain the previously noted variability in dissociation rate of **5**, whose half-life we found to increase by an order of magnitude when its concentration was raised from near-zero to 1 mM, and provide mechanistic insight into the factors that govern dissociation rates among diazeniumdiolates of importance as pharmacologic progenitors of NO.

Introduction

Many recent studies have established that nitric oxide (NO) is an important bioregulatory agent in a range of physiological processes from vasodilation and platelet aggregation to neurotransmission and penile erection.[1−4] In support of the widespread interest and activity which have arisen in nitric oxide biochemistry, there has followed a need for compounds which can conveniently deliver NO to biological systems at physiological pH.[5] Diazeniumdiolate ions of structure **1**, adducts of nitric oxide with secondary amines,[6] hydrolyze to NO in aqueous media and thus constitute a versatile class of nitric oxide donors for pharmacological research applications as well as promising lead compounds for drug discovery.[7,8]

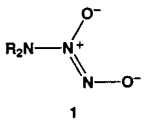

1

It has been previously demonstrated that diazeniumdiolates dissociate spontaneously at rates that vary widely depending on their structure and the pH of the reaction medium.[9,10] Although most applications for diazeniumdiolates are at physiological pH, the manner in which their dissociation rates depend on the pH of the solution is of considerable interest, both for practical reasons related to their stability during preparation and storage and because of the important mechanistic information it can provide. Such information is directly relevant to their many pharmacological applications and to their employment in studies exploring the chemical biology of nitric oxide.[11] The selective in vivo application of diazeniumdiolates in regions of lowered pH (e.g., in many tumors) would also require detailed

* Address correspondence to this author. Phone: 703-993-1075. Fax: 703-993-1055. E-mail: kdavies @gmu.edu.

† George Mason University.

‡ National Cancer Institute.

§ SAIC Frederick.

(1) *Nitric Oxide Part C: Biological and Antioxidant Activities*; Methods in Enzymology, Vol. 301; Academic Press : San Diego, 1999; pp 3−589.

(2) *The Biology of Nitric Oxide, Part 7*; Portland Press: London, 2000.

(3) *Pathophysiology and Clinical Application of Nitric Oxide*; Harwood Academic Publishers: Amsterdam, The Netherlands, 1999.

(4) *Nitric Oxide and the Cardiovascular System*; Humana Press: Totowa, NJ, 2000.

(5) Keefer, L. K. *Pharm. News* **2000**, *7*, 27−32.

(6) Drago, R. S. Reactions of nitrogen(II) oxide. In *Free Radicals in Inorganic Chemistry*; Colburn, C. B., Ed.; Adv. Chem. Ser. No. 36; American Chemical Society: Washington, DC, 1962; pp 143−149.

(7) Keefer, L. K. *CHEMTECH* **1998**, *28*, 30−35.

(8) Saavedra, J.; Keefer, L. *Chem. Br.* **2000**, *36*, 30−33.

(9) Maragos, C. M.; Morley, D.; Wink, D. A.; Dunams, T. M.; Saavedra, J. E.; Hoffman, A.; Bove, A. A.; Isaac, L.; Hrabie, J. A.; Keefer, L. K. *J. Med. Chem.* **1991**, *34*, 3242−3247.

(10) Keefer, L. K.; Nims, R. W.; Davies, K. M.; Wink, D. A. *Methods Enzymol.* **1996**, *268*, 281−293.

(11) Wink, D. A.; Mitchell, J. B. *Free Radical Biol. Med.* **1998**, *25*, 434−456.

10.1021/ja002899q CCC: $20.00
Published on Web 04/19/2001

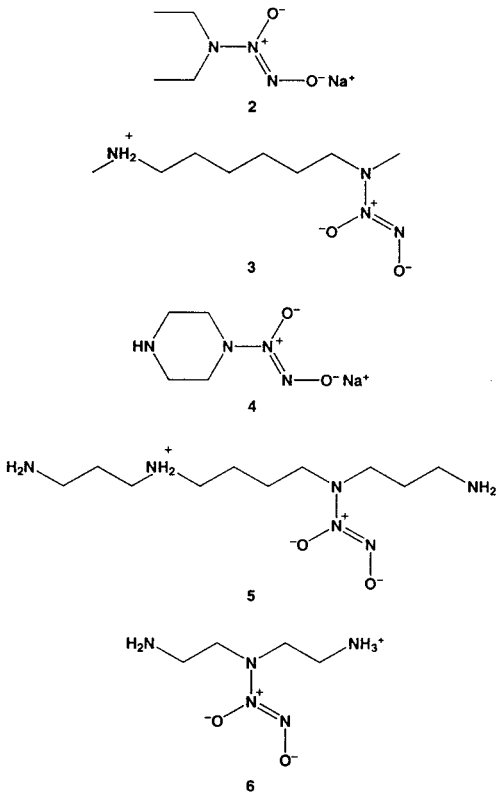

Figure 1. Structures of diazeniumdiolates included in this investigation.

knowledge of their pH/rate profiles. Such knowledge is necessary if steep pH versus rate dependences are to be successfully exploited in the selective activation of systemically administered diazeniumdiolates.

In this paper we report a detailed investigation of the decomposition of diazeniumdiolates **2**−**6** derived from *N*,*N*-diethylamine, *N*,*N*′-dimethyl-1,6-hexanediamine, piperazine, spermine, and diethylenetriamine, respectively, whose structures are shown in Figure 1. Our findings illustrate the varied reaction chemistry which can follow the structural variations exhibited by these compounds.

Results and Discussion

pH Dependence of Diazeniumdiolate Dissociation Rates. The dissociation reactions of diazeniumdiolates **2**−**6** follow simple pseudo-first-order rate laws, with the measured first-order rate constant, k_{obs}, dependent on the pH of the solution. In all cases, the rate data and spectral changes obtained are consistent with an acid-catalyzed decomposition of the $[N(O)NO]^-$ group yielding the parent amine with release of nitric oxide. For **2** and **3**, the kinetic data (Table 1) indicate a single protonation in the pH range studied (eqs 1−3), while with **4**, **5**, and **6**, a more complex dependence on pH is found, implicating more than one kinetically significant protonation state of the substrate in the decomposition.

$$\mathbf{1}\cdot H^+ \overset{K_{AH}}{\rightleftharpoons} \mathbf{1} + H^+ \quad (1)$$

$$\mathbf{1}\cdot H^+ \xrightarrow{k_{AH}} R_2NH + 2NO \quad (2)$$

$$k_{obs} = k_{AH}[H^+]/([H^+] + K_{AH}) \quad (3)$$

Kinetic Data for Compounds 2 and 3. The linear plots of k_{obs} versus $[H^+]$ passing through the origin (Figure A, Supporting Information) found for **2** and **3** are consistent with their dissociations proceeding through unimolecular decay of the diazeniumdiolate following equilibrium protonation of the substrate (eqs 1 and 2). Rate and equilibrium parameters were obtained by fitting pH−rate data to linear forms of eq 3 through plots of $1/k_{obs}$ versus $1/[H^+]$. Individual k_{AH} and pK_{AH} values for **2** of (1.11 ± 0.44) s^{-1} and (5.04 ± 0.17), respectively, and for **3** of (0.518 ± 0.392) s^{-1} and (5.88 ± 0.35), respectively, were obtained from the linear dependence of $1/k_{obs}$ on $1/[H^+]$, which was apparent in the lower pH solutions.

Table 1. pH Dependence of First-Order Rate Constants for Dissociation of **2** and **3** in 0.10 M Phosphate Buffer at 37.0 °C[a]

2		**3**	
pH	k_{obs} (s^{-1})	pH	k_{obs} (s^{-1})
8.00	0.00215	12[b]	8.2×10^{-7}
7.80	0.00345	10[c]	0.000810
7.56	0.00438	8.00	0.00483
7.40	0.00585	7.82	0.00661
6.95	0.0127	7.56	0.0105
6.55	0.0281	7.42	0.0167
6.48	0.0367	6.95	0.0397
6.20	0.0711	6.55	0.0944
6.07	0.0972		
5.81	0.156		
5.64	0.200		
5.45	0.32		
5.16	0.568		

[a] [Diazeniumdiolate] = 0.10 mM. [b] 1×10^{-2} M NaOH. [c] 1×10^{-4} M NaOH.

Table 2. pH Dependence of First-Order Rate Constants for Dissociation of **4** and **4a** in 0.10 M Phosphate Buffer at 37 °C[a]

4		**4a**	
pH	k_{obs} (s^{-1})	pH	k_{obs} (s^{-1})
8.50	0.00114	7.56	0.00351
8.04	0.00152	6.95	0.00875
7.80	0.00172	6.07	0.0191
7.56	0.00190	5.64	0.0527
7.40	0.00258		
6.95	0.00285		
6.55	0.00489		
6.19	0.00763		
6.07	0.00706		
5.81	0.0120		
5.64	0.0134		
5.62	0.0169		
5.43	0.0232		
5.16	0.0341		

[a] [Diazeniumdiolate] = 0.10 mM.

Diazeniumdiolates Derived from Piperazine and Spermine. The more complex rate dependence on acidity that was found with both **4** and **5** (Tables 2 and 3) is consistent with their dissociations proceeding to products through more than one reaction path. For **4**, a departure from linearity in the plot of k_{obs} versus $[H^+]$ was observed at the highest pH values studied (Figure B, Supporting Information), while the data for **5** showed a linear dependence on $[H^+]$ over the whole pH range (Figure 2). In both cases, the plots had a significant nonzero intercept. The relation $k_{obs} = a + b[H^+]$, describing the linear dependence on $[H^+]$, is a limiting form of the two-term rate law (eq 4), which applies when $K_{AH} \gg [H^+]$. This is apparent between pH 7.4 and 5.4 for **4** and between 8.5 and 6.1 for **5**.

Equation 4 also identifies the term *a* as k_A and *b* as k_{AH}/K_{AH}. The k_A value is obtained from the intercept of the plot of k_{obs} versus $[H^+]$. Individual values for k_{AH} and K_{AH} are obtained from eq 5, the linear form of eq 4, through the plot of $1/(k_{obs} -$

Table 3. Dependence of First-Order Rate Constants for Dissociation of **5** on Substrate Concentration and pH in 0.10 M Phosphate Buffer at 37 °C

pH 7.4		pH 5.6			
[**5**] (μM)	k_{obs} (s^{-1})	[**5**] (μM)	k_{obs} (s^{-1})	pH[a]	k_{obs} (s^{-1})[a]
				8.50	0.000735
				8.04	0.000736
12.6	0.00201			7.82	0.00079
23.5	0.00152			7.56	0.00074
100	0.00107[b]	8.5	0.00549	7.42	0.00078
107	0.00115	18.4	0.00563	6.95	0.00118
220	0.000713	43.3	0.00657	6.55	0.00172
295	0.000550	87.4	0.00576	6.2	0.00295
403	0.000449	182	0.00579	6.07	0.00353
759	0.000326			5.8	0.0048
988	0.000249			5.64	0.00688
				5.60	0.00746

[a] [**5**] = 1×10^{-4} M. [b] Mean value of eleven measurements at [**5**] = 0.10 mM using four different preparations of **5** (standard deviation = 1.2×10^{-4} s^{-1}).

k_A) versus 1/[H^+], for data obtained in the more acidic solutions.

$$k_{obs} = \frac{k_{AH}[H^+] + k_A K_{AH}}{[H^+] + K_{AH}} \quad (4)$$

$$\frac{1}{k_{obs} - k_A} = \frac{K_{AH}}{(k_{AH} - k_A)[H^+]} + \frac{1}{k_{AH} - k_A} \quad (5)$$

The nonlinear dependence of k_{obs} on [H^+] observed in measurements of **4**'s dissociation rate made above pH 7.4 is consistent with the existence of a second reaction path initiated by a protonation of the substrate in the higher pH solutions. Specific rate and equilibrium constants associated with this path are realized through the rate equation (eq 6), which describes the dissociation of **4**, through both mono- and diprotonated forms of the substrate, over the whole pH range examined.

$$k_{obs} = \frac{k_{AH}[H^+]^2 + k_A K_{AH}[H^+]}{[H^+]^2 + K_{AH}[H^+] + K_{AH}K_A} \quad (6)$$

Equation 4, describing the reaction of **4** below pH 7.4, is a limited form of eq 6, which reduces to eq 4 in the more acidic solutions.

A fit of the data obtained for **4** to eq 6 is illustrated in Figure 3, in which k_{obs} values are plotted against the reaction pH and compared with values calculated by eq 6 using the rate and equilibrium parameters $K_{AH} = (1.29 \pm 0.86) \times 10^{-5}$ M, $K_A = (5 \pm 1) \times 10^{-9}$ M, $k_{AH} = (0.091 \pm 0.062)$ s^{-1}, and $k_A = (2.19 \pm 0.98) \times 10^{-3}$ s^{-1}. The value of K_A was estimated from the best fit of k_{obs} values to values calculated with eq 6, using the K_{AH}, k_{AH}, and k_A values indicated above. The close fit of the observed and calculated values over the whole pH range studied lends support to the proposed mechanism and the individual rate and equilibrium values obtained.

Scheme 1 illustrates the dissociation of **4** through both mono- and diprotonated forms of the substrate. The pK_A of 8.3 compares to the literature pK_a values of 9.8 and 11.1 for monoprotonated piperazine and piperidine, respectively,[12] and is attributed to protonation of the remote piperazine nitrogen in **4** (i.e., the one not carrying the diazeniumdiolate functional group; see Scheme 1). At pH 7.4, it is this protonation that controls the major pathway to NO release, with some 85% of the reaction proceeding through the k_A path. The constraints imposed by the piperazine ring structure would facilitate a rapid proton transfer between the nitrogen sites, thereby enabling the initial protonation at the remote piperazine nitrogen to influence the decomposition of the diazeniumdiolate group; no such effect was detected for **3**, whose remote basic site is six carbons removed from the diazeniumdiolate group. With **4a**, only one dissociation pathway was found and measured k_{obs} values showed a linear dependence on [H^+] passing through the origin. In this case, the reduced basicity of the second nitrogen apparently inhibits the protonation of the remote nitrogen and activation of the [N(O)NO]$^-$ group by a similar mechanism.

(12) *Dictionary of Organic Compounds*; Chapman & Hall: London, 1996; p 5380.

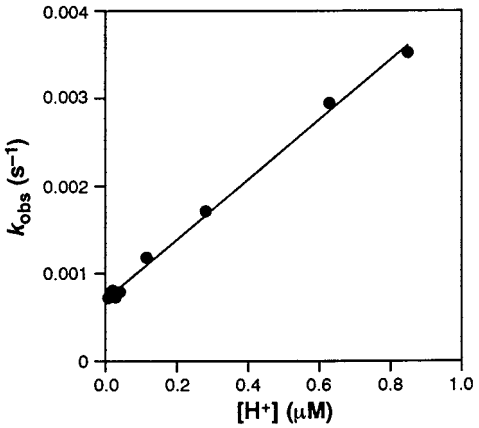

Figure 2. Plot of k_{obs} versus [H^+] between pH 6.1 and 8.5 for 0.10 mM **5** in 0.10 M phosphate buffer at 37 °C.

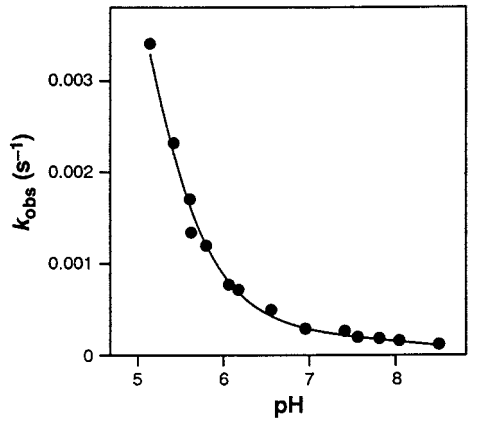

Figure 3. Measured first-order rate constants (●) for decay of **4** in 0.10 M phosphate buffer at 37 °C. Expected values calculated by eq 6 where $K_{AH} = 1.3 \times 10^{-5}$ M, $K_{AH} = 5 \times 10^{-9}$ M, $k_{AH} = 0.0907$ s^{-1}, and $k_A = 0.0022$ s^{-1} are represented by the solid curve.

Scheme 1

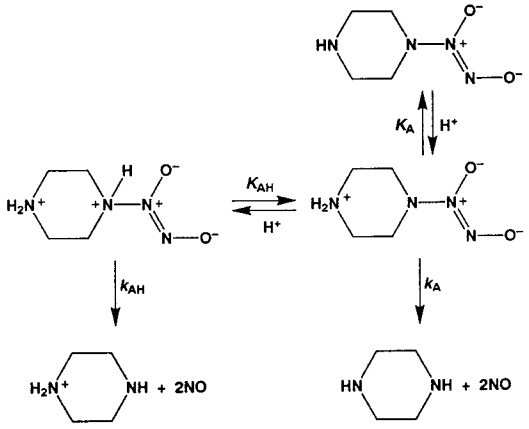

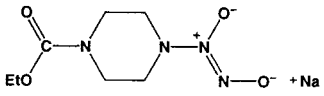

4a

In the lower pH solutions, equilibrium protonation of both ring nitrogens occurs, leading to more rapid decomposition through the k_{AH} path. The pK_{AH} value of 4.9 for the second protonation of **4** compares to the pK_a value of 5.4 for diprotonated piperazine.

Corresponding K_{AH}, k_{AH}, and k_A values obtained for the zwitterionic diazeniumdiolate **5**, derived from spermine, are $(3.19 \pm 1.55) \times 10^{-6}$ M, (0.0138 ± 0.0064) s^{-1}, and $(7.2 \pm 1.5) \times 10^{-4}$ s^{-1}, respectively. With **5**, the k_A pathway is presumably initiated by a separate equilibrium protonation of the substrate occurring in the higher pH solutions. This event was not detected kinetically in the pH range studied. pK_a values of 8.60, 9.33, 10.45, and 11.23,[11] reported for spermine, would suggest the existence of a suitably basic site in **5**.[13]

Concentration Dependence in Kinetic Data for a Polyamine Derivative 5. The zwitterionic diazeniumdiolate **5**, formed from the polyamine spermine, displayed a further complexity in its kinetic behavior beyond that found with all others studied. At pH 7.4, first-order rate constants obtained from the linear regression of $\ln(A_t - A_\infty)$ plots displayed a dependence on the concentration of **5** employed in the reaction, with the apparent half-life increasing from 5.7 to 46 min as the initial substrate concentration was varied from 1.3×10^{-5} to 9.9×10^{-4} M. Rate data were also obtained at 0.10 mM substrate levels as a function of pH between 8.5 and 5.6. Data are summarized in Table 3.

The observed rate inhibition at high substrate concentration is consistent with a reaction scheme in which **5** is partitioned into an unreactive dimerized form at pH 7.4, with the dimer and monomer at equilibrium (eq 7) and with the dissociation to NO proceeding through both the monomer, S, and its conjugate acid (eq 8). The concentration of monomer S present

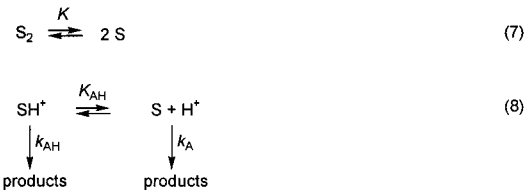

(7)

(8)

at equilibrium is given in eq 9, which is obtained from solution of the quadratic expression[14] generated from eq 7 and the mass balance expression $S_T = [S] + 2[S_2]$, where S_T is the total formal concentration of **5** employed in the reaction.

$$[S] = \frac{2S_T}{([8S_T/K] + 1)^{1/2} + 1} \tag{9}$$

$$-dS_T/dt = (k_A + k_{AH}[H^+]/K_{AH})[S] = \frac{2(k_A + k_{AH}[H^+]/K_{AH})S_T}{[(8S_T/K) + 1]^{1/2} + 1} \tag{10}$$

Combining eq 10 (which follows from eqs 8 and 9) with the experimentally determined rate dependence on **5**, $-dS_T/dt = k_{obs}S_T$, gives eq 11; this suggests that the observed first-order rate constants, k_{obs}, should decrease with increase in substrate concentration, S_T, as has been found. Equations 12 and 13 follow in the limit that $(8S_T/K)^{1/2} \gg 1$.

$$k_{obs} = \frac{2(k_A + k_{AH}[H^+]/K_{AH})}{[(8S_T/K) + 1]^{1/2} + 1} \tag{11}$$

$$-dS_T/dt = (K/2)^{1/2}(k_A + k_{AH}[H^+]/K_{AH})S_T^{1/2} \tag{12}$$

$$k_{obs} = (K2S_T)^{1/2}(k_A + k_{AH}[H^+]/K_{AH}) \tag{13}$$

The overall order with respect to the substrate concentration was confirmed by measuring initial rates R_o as a function of initial concentration, S_T. Initial rates were obtained by multiplying the initial concentration by the measured first-order rate constants, k_{obs} (i.e., $R_o = k_{obs}S_T$). This is a more precise way of obtaining values of initial rates than measuring initial gradients of A_t versus t plots, even if the reaction is not first-order in [**5**]. The plot of $\log(k_{obs}S_T)$ versus $\log S_T$ has a gradient of 0.53 ± 0.04.

$$-dS_T/dt = (k_A + k_{AH}[H^+]K_{AH})S_T \tag{14}$$

In the limit of low concentration, which is realized when $8S_T/K \ll 1$, eq 14 would apply; under these conditions, the equilibrium is shifted completely in favor of the monomer.

At pH 7.4 a dimer of **5**, formed through a head-to-tail association of an anionic diazeniumdiolate functional group and one of the cationic sites of a given monomer zwitterion with those of another, would not be unexpected. The polyammonium ions derived from spermine, the parent polyamine, are known to have high affinity for the polyanionic nucleic acids at physiological pH values, and interactions between ammonium groups and donor atoms on both the bases and the phosphates have been implicated in these associations.[13] In reactions between spermine and phosphoimidazolide analogues of guanosine triphosphate, rate reductions observed at high pH have been attributed to the association between protonated and deprotonated spermine species that occur when the concentrations of the protonated and deprotonated amines become comparable in the higher pH solutions.[13] The presence of the anionic $[N(O)NO]^-$ functional group in **5** would be expected to enhance its self-association beyond that found for spermine.

At lower pH, the increased acidity is expected to inhibit the dimerization by protonation of the diazeniumdiolate functional group and/or multiple protonation of the amine sites. At pH 5.6, first-order rate constants for the dissociation of **5** did not exhibit the dependence on substrate concentration that was found at pH 7.4. The value of the measured first-order rate constant, $k_{obs} = (5.93 \pm 0.35) \times 10^{-2}$ s^{-1}, was independent of five initial substrate concentrations employed between 8.5×10^{-6} and 1.8×10^{-4} M.

In light of the unusual kinetic behavior displayed by **5**, the possibility of modulating the dissociation rates of **5** by trace metal ions was also explored. Metal ion interactions with the $[N(O)NO]^-$ functional group and with the amine nitrogen sites of the **5** molecule both present themselves as possible routes to metal ion interference. Possible rate effects arising from the presence of spermine and nitrite ion, the two most likely impurities in samples of **5**, were also examined.

The dissociation rates of **5** were measured in the presence of a series of trivalent and divalent metal salts, $FeCl_3$, $Al(NO_3)_3$, $La(NO_3)_3$, $CaCl_2$, $ZnCl_2$, and $MgSO_4$. Ferric salts were found

(13) Kanavarioti, A.; Baird, E. E.; Smith, P. J. *J. Org. Chem.* **1995**, *60*, 4873−4883.

(14) Espenson, J. H. An Intermediate Which Reacts in Steps Having Different Reaction Orders. In *Chemical Kinetics and Reaction Mechanisms*; Ricci, J., Bradley, J. W., Eds.; McGraw-Hill: New York, 1981; pp 79−80.

Table 4. Effect of Added Metal Ions on the Dissociation Rate of **5** at 37 °C and pH 7.4[a]

	$[M^{n+}]$ (μM)	k_{obs} (s^{-1})	$t_{1/2}$ (min)
$[Fe^{3+}]$[b]	105[c]	0.00056	21
	100	0.00059	20
	100	0.00040	29
	100	0.00056[d]	23
	100	0.00060[d]	19
	98.5	0.00058	20
	57.5	0.00075	15
	29.0	0.00088	13
	10.0	0.00101	11
	0.00[c]	0.00107[e]	10.8 ± 2.1
$[Cu^{2+}]$	100	0.00066	17.5
$[La^{3+}]$	100	0.00081	14.3
$[Al^{3+}]$	100	0.00090	12.8
$[Ca^{2+}]$	100	0.00092	12.5
$[Zn^{2+}]$	500	0.00115	10.0
$[Mg^{2+}]$	108	0.00134	8.6

[a] Except as otherwise indicated, reactions were run in 0.10 M phosphate buffer; [**5**] = 0.10 mM. [b] $FeNH_4(SO_4)_2 \cdot 12H_2O$ except where indicated. [c] $FeCl_3 \cdot 6H_2O$. [d] 0.050 M Tris buffer. [e] Mean value, (0.00107 ± 0.00012) of eleven measurements at [**5**] = 0.10 mM.

to have the most significant influence on the rate. Although ferric ion had no effect on the dissociation rate when present at trace levels, it produced an appreciable rate inhibition when added at concentrations approaching that of the substrate. First-order rate constants decreased progressively with increase in [Fe(III)] from 0.020 to 0.10 mM, resulting in a doubling of the half-life (relative to the metal-free system) when **5** and iron(III) were together at 0.10 mM concentrations. Good first-order behavior was apparent with [Fe(III)] in the above concentration range, although departure from linearity in the first-order plots was noticeable at higher ferric ion concentrations. Similar behavior was noted with either $FeCl_3 \cdot 6H_2O$ or $Fe(NH_4)(SO_4)_2 \cdot 12H_2O$ as the iron(III) source, and also with either 0.10 M phosphate or 0.050 M Tris employed as the buffer medium. Data obtained are summarized in Table 4.

Because of the possibility of an apparent rate inhibition resulting from light scattering (rather than inhibition by the iron complex) by $Fe(OH)_3$ or other insoluble hydrated iron(III) species, repetitive spectral scans, between 200 and 500 nm, were conducted on a 1×10^{-4} M solution of Fe^{3+} alone in pH 7.4 phosphate buffer. Spectra obtained were, however, unchanged over 40 min although stock solutions of 10 mM Fe^{3+} in water did become cloudy on standing for periods of greater than about 1 h.

Rate inhibition by iron(III) appears to be a characteristic of **5** alone. The dissociation of **2** and **3** in the presence of equimolar ferric nitrate resulted in less than 8% change in the measured rate constant, which is close to the normal precision of spectrophotometrically determined reaction rates of diazeniumdiolate substrates.

A 38% reduction in the measured first-order rate constant was observed with Cu(II) added. This was somewhat smaller than that found with Fe(III) (ca. 60%) at comparable concentrations. Other metal salts, $Al(NO_3)_3$, $La(NO_3)_3$, $CaCl_2$, and $ZnCl_2$, when present in 0.1 mM solutions of **5** at comparable concentrations, produced rate reductions of less than 20%, as compared to duplicate experiments carried out with no metal present. Magnesium sulfate resulted in a 13% increase in the measured rate constant.

The most likely source of the ferric ion-induced rate inhibition is through the formation of an unreactive Fe(III)-**5** adduct by equilibrium association of the **5** anion with Fe^{3+} or other iron(III) species present in the solution. For such an event, the reaction rate is expected to decrease at higher iron concentrations as **5** is increasingly partitioned into the unreactive Fe(III)-adduct form (eq 15). (A plot of $1/k_{obs}$ versus [Fe(III)] consistent with

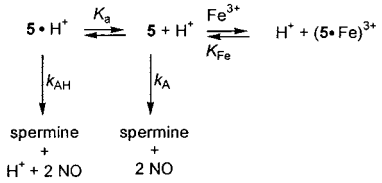

(15)

this mechanism is shown in Figure C, Supporting Information.) Several association species involving Fe^{3+} interaction with the **5** amine nitrogens and/or the oxygens of the $[N(O)NO]^-$ functional group can be envisaged, although the known preference of ferric ion for oxygen donor ligands would favor the diazeniumdiolate oxygens as the coordination site to the metal. The anionic $R_2N[N(O)NO]^-$ functional group is known to coordinate metal centers and several copper complexes have been characterized.[15−18] Since some association is expected between ferric ion and the hydrogen phosphate and dihydrogen phosphate species present in phosphate buffer at pH 7.4, the finding of a similar rate inhibition in both Tris and phosphate buffers suggests that the anionic $[N(O)NO]^-$ functional group is able to compete effectively with phosphate ions for coordination sites on the metal, possibly because of its ability to chelate the metal. The origin of the relatively small rate effects noted with the other metal ions is also assumed to be due to interaction with the diazeniumdiolate functional group, although they have not been examined in any detail. The selectivity displayed by **5** for iron(III), as compared to other metal ions tested, does not appear to be tied to the size of the metal.

Attempts at finding spectral evidence for an Fe(III)-**5** association species were unsuccessful. Repetitive scans between 200 and 500 nm of equimolar (1×10^{-4} M) Fe^{3+} and **5** in 0.10 M phosphate buffer at pH 7.4 showed no evidence for any absorbing species other than the two reactants. Similar experiments at millimolar concentration levels were inconclusive due to precipitation of $Fe(OH)_3$.

The effect on the rate of the two most likely impurities in the **5** sample, spermine and nitrite, was also examined. Spermine, the parent polyamine, when added at concentrations up to 10 times the **5** levels, had no effect on the reaction rate. Nitrite ion has previously been shown[19] to affect the decomposition rate of the related diazeniumdiolate, Angeli's salt, NaO[N(O)NO]Na. Sodium nitrite did result in an increase in the **5** dissociation rate, though only when added at fairly high concentrations. A 67-fold increase in the nitrite concentration from 1.5 mM to 0.10 M produced a 24% increase in the **5** dissociation rate. Rate changes of similar magnitude were, however, noted in experiments exploring ionic strength effects, and the nitrite's effect on the rate most likely has a similar origin. A 50-fold increase in the total phosphate buffer concentration from 2.0 to 100 mM produced a 33% increase in the **5**

(15) Christodoulou, D.; George, C.; Keefer, L. K. *J. Chem. Soc., Chem. Commun.* **1993**, 937−939.

(16) Christodoulou, D.; Maragos, C. M.; George, C.; Morley, D.; Dunams, T. M.; Wink, D. A.; Keefer, L. K. Mixed-ligand, non-nitrosyl Cu(II) complexes as potential pharmacological agents via NO release. In *Bioinorganic Chemistry of Copper*; Karlin, K. D., Tyeklár, Z., Eds.; Chapman & Hall: New York, 1993; pp 427−436.

(17) Schneider, J. L.; Young, V. G., Jr.; Tolman, W. B. *Inorg. Chem.* **1996**, *35*, 5410−5411.

(18) Schneider, J. L.; Halfen, J. A.; Young, V. G., Jr.; Tolman, W. B. *New J. Chem.* **1998**, *22*, 459−466.

(19) Hughes, M. N.; Wimbledon, P. E. *J. Chem. Soc., Dalton Trans.* **1977**, 1650−1653.

Table 5. Effect of Spermine and Sodium Nitrite on the Dissociation of **5** at 37 °C and pH 7.4[a]

[spermine] (mM)	k_{obs} (s^{-1})	$t_{1/2}$ (min)	[$NaNO_2$] (mM)	k_{obs} (s^{-1})	$t_{1/2}$ (min)
0.11	0.00086	13.4	0.00	0.000836	13.8
0.41	0.00081	14.3	0.105	0.000762	15.1
0.97	0.00085	13.6	0.210	0.000732	15.8
			0.400	0.000636	18.1
			1.00	0.000588	19.2
			1.52	0.000633	18.2

[a] [**5**] = 0.10 mM in 0.10 M phosphate buffer.

Table 6. Effect of Buffer Medium and Buffer Concentration on First-Order Rate Constants for Dissociation of Diazeniumdiolates at 0.1 mM Concentration at 37 °C and pH 7.4

	$[PO_4]_T$ [a] (M)	k_{obs} (s^{-1})	pH[b]
2	0.50	0.00609	7.36
	0.10	0.00544	7.44
	0.010	0.00528	7.43
	0.002	0.00485	7.56
3	0.10	0.0161	7.37
	0.020	0.0114	
	0.010	0.00860	7.38
	0.0050	0.00860	
	0.0020	0.00765	7.38
4	0.10	0.00318	7.36
	0.010	0.00286	7.42
	0.0020	0.00296	7.50
5	0.10	0.00112	7.38
	0.010	0.00095	7.43
	0.0050	0.00084	7.43
	[Tris][c] (M)	k_{obs} (s^{-1})	pH
3	0.050	0.0128	7.41
4	0.050	0.00365	7.42
5	0.050	0.00089	7.42

[a] [NaH_2PO_4] + [Na_2HPO_4]. [b] Measured pH of reaction solution. [c] [Tris hydrochloride] + [Tris base].

dissociation rate. Ionic strength effects of similar magnitude were also found with all other diazeniumdiolates studied. Reaction rates measured in Tris buffers showed only minor differences from those obtained in phosphate media. Details of the spermine, nitrite, and ionic strength effects are summarized in Tables 5 and 6.

Kinetics of Dissociation of 6, an Especially Long-lived Ionic NO Generator. The zwitterion **6**, derived from the polyamine diethylenetriamine, exhibits the slowest NO release rate ($t_{1/2}$ ~20 h at 37 °C and pH 7.4) of all diazeniumdiolate ions studied to date.[10] The longer half-lives for its acid-catalyzed dissociation have enabled its reaction behavior to be monitored over a much wider pH range (7.4−2.0) than was possible with the other more rapidly reacting NO donors. Rate data for **6** obtained over this extended pH range, summarized in Table 7, have revealed the existence of two separate acid-catalyzed decay paths. First-order rate constants measured in phosphate buffers between pH 7.46 and 5.88, when fitted to eq 3, yielded rate and equilibrium parameters, $k_{AH} = (2.75 \pm 1.75) \times 10^{-4}$ s^{-1} and $pK_{AH} = 5.94 \pm 0.31$, for the acid-catalyzed path operating at higher pH. When measurements were extended to lower pH, k_{obs} values increased again between pH 4.0 and 2.5, before leveling off as the reaction pH approached 2 (Figure D, Supporting Information). Reciprocal plots of $1/k_{obs}$ against $1/[H^+]$ for data obtained between pH 2.04 and 5.04 showed excellent linearity, consistent with the second acid-catalyzed path in this low-pH region. Linear regression of the $1/k_{obs}$ versus $1/[H^+]$ plot yielded $k_{AH2} = (0.0333 \pm 0.0310)$ s^{-1} and $pK_{AH2} = 3.09 \pm 0.42$. Confirmation of a separate reaction pathway

Table 7. Rate Data for the Dissociation of 0.10 mM **6** in Buffered Aqueous Solutions at 37 °C

pH	k_{obs} (s^{-1})	$t_{1/2}$	buffer
7.46	7.98×10^{-6}	24.1 h	Na_2HPO_4/NaH_2PO_4
7.24	1.42×10^{-5}	13.6 h	
7.08	1.87×10^{-5}	10.3 h	
6.80	3.17×10^{-5}	6.1 h	
6.31	7.43×10^{-5}	2.6 h	
6.08	1.03×10^{-4}	1.9 h	
5.88	1.63×10^{-4}	1.2 h	
5.04	6.31×10^{-4}	18.3 min	CH_3CO_2Na/CH_3CO_2H
4.50	2.06×10^{-3}	5.6 min	
4.47	2.37×10^{-3}	4.9 min	
3.85	5.82×10^{-3}	2.0	
3.44	9.72×10^{-3}	1.2 min	
3.43	0.0119	58 s	Glycine/HCl
3.30	0.0152	46 s	
3.17	0.0146	47 s	
2.99	0.0140	50 s	
2.81	0.0245	28 s	
2.56	0.0222	31 s	
2.42	0.0264	26 s	
2.04	0.0295	24 s	

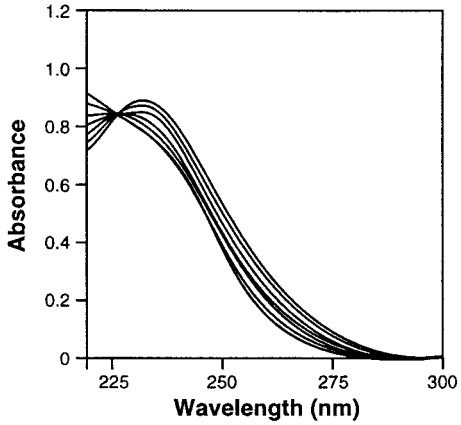

Figure 4. Spectral changes accompanying the dissociation of **6**. Spectra were recorded 10, 16, 25, 37, 52, 80, and 260 s after dissolution in 0.05 M glycine hydrochloride buffer at pH 2.5 and 37 °C.

for the decomposition of **6** is provided in the spectral data (Figure 4), which show the reaction proceeding through the decay of the 230-nm absorption maximum that characterizes **6** at pH 2.5.

A summary of the individual rate and equilibrium constants obtained for compounds **2**−**6** is given in Table 8.

Spectrally Determined pK_a Values. An absorption maximum at 250−254 nm was found to be characteristic of ionic diazeniumdiolates **2**−**6** whether in sodium hydroxide solution or in phosphate buffers at pH 7.4. At lower pH, a shift in the absorption maximum to 228−232 nm was noted in each case. The plot of λ_{max} versus pH displayed a sigmoidal curve, with the sharp transition to lower wavelengths occurring at a pH characteristic of the particular diazeniumdiolate substrate. Typical plots are shown in Figure 5. The rapid shift in λ_{max} when pH was lowered was noted before a significant drop in absorbance had occurred, consistent with protonation of the $[N(O)NO]^-$ chromophore prior to decomposition of the substrate. The midpoint in the transition from ~250 nm (pH 8−5.5) to ~230 nm (pH 2.5−1.8) yielded estimates of the spectral pK_a. Values obtained with the diazeniumdiolates **2**, **3**, **4**, **5**, and **6** were 4.5, 4.6, 4.2, 3.5, and 3.1, respectively. The uncertainty associated with these pK_a values is estimated as ≤0.2.

The spectrally determined pK_a values for compounds **2**−**6** are summarized in Table 8.

Table 8. Summary of Rate Parameters for Nitric Oxide Dissociation and Kinetic and Spectral pK_a Values for Protonation of Compounds **2**−**6**

substrate	k_A (s^{-1})	pK_A	k_{AH} (s^{-1})	pK_{AH}	k_{AH2} (s^{-1})	pK_{AH2}	spectral pK_a
2			1.1 ± 0.4	5.0 ± 0.2			4.5 ± 0.2
3			0.52 ± 0.39	5.9 ± 0.3			4.6 ± 0.2
4	$(2.2 \pm 1.0) \times 10^{-3}$	8.3 ± 0.1	0.091 ± 0.062	4.9 ± 0.3			4.2 ± 0.2
5	$(7.2 \pm 1.5) \times 10^{-4}$		0.014 ± 0.006	5.5 ± 0.2			3.5 ± 0.2
6			$(2.8 \pm 1.8) \times 10^{-4}$	5.9 ± 0.3	0.033 ± 0.031	3.1 ± 0.4	3.1 ± 0.2

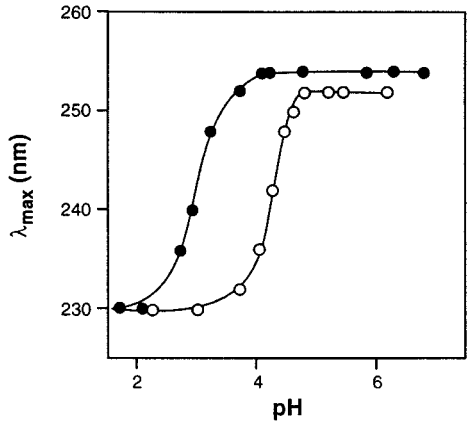

Figure 5. Variation of λ_{max} for **4** (○) and **6** (●) as a function of solution pH.

Protonation States Involved in NO Generation. In all the cases we have studied, the kinetic data demonstrate that hydrogen ion initiates the diazeniumdiolate dissociation reaction, with equilibrium protonation of the substrate preceding release of NO. Of interest, therefore, is the site (or sites) of protonation that triggers the decomposition of the $[N(O)NO]^-$ functional group, and the mechanism by which NO is obtained. With **4**, **5**, and **6**, two successive protonations of kinetic significance were identified from the rate data, while with **2** and **3**, a single protonation event was detected kinetically within the pH ranges employed.

In an effort to decipher which specific protonation states are responsible for the observed dissociation reactions, we have compared the spectrally derived pK_a values reported in the previous section with values obtained through the kinetic data. To assess the origin of our observed proton-induced spectral shifts, we have compared them with the spectral data of Table 9, which summarizes the closely similar electronic spectral characteristics for the two ions $X[N(O)NO]^-$, where X = Me or Me_2N, together with those of their known methyl derivatives. The similarity of spectra for the two XN(O)═NOMe derivatives invites the assumption that the spectra of the two as-yet-unknown $Me_2N[N(O)NO]Me$ isomers would be similar to those of the corresponding Me[N(O)NO]Me analogues. With the further assumption that methylation and protonation of the $X[N(O)NO]^-$ chromophore should lead to similar spectral changes for all mesomerically inactive substituents X, the data of Table 9 should provide a reasonable guide for inferring the kinetically significant position(s) of protonation in the dissociation of ions **2**−**6**.

Taking **6** as an example, we have examined its ultraviolet spectral characteristics as the pH of its solutions was lowered through its two kinetically identified pK_a values (5.94 and 3.09). Ultraviolet data for analogous diazeniumdiolates (Table 9) suggest that protonation anywhere within the $[N(O)NO]^-$ group (i.e., at O1, N2, or O2 of structure **1′**) should induce a substantial shift in the absorbance maximum in one direction or the other. As shown in Figure 5, no such change was observed on lowering the pH through the higher pK_a of **6**. We thus infer that O1, N2, and O2 are not significantly protonated in the pH range of 4 to 7, and that the reaction path followed at pH >4 must proceed through tautomer A of Scheme 2. Catalysis by protonating the R_2N nitrogen is easily rationalized in terms of the greater suitability of R_2NH as a leaving group relative to R_2N as well as the juxtaposition of electropositive nitrogens in tautomer A arising from the partial double bond character of the N1−N2 linkage.[20,21]

Table 9. Ultraviolet Spectral Characteristics of Selected $X[N(O1)N2O2]^-$ Ions and Their Alkylated Derivatives[a]

	λ_{max} (ϵ)			
X	free anion	methylated on O1	methylated on N2	methylated on O2
Me_2N	250 (7.6)[b]	*c*	*c*	234 (6.8)[b]
Me	248 (8.6)[d]	232 (5.2), 338 (0.086)[d]	265 (10.0)[e]	234 (8.3)[f]

[a] Data are for aqueous solutions with λ_{max} being given in nm and ϵ in $mM^{-1}\ cm^{-1}$. [b] Data from ref 32. [c] Isomer unknown. [d] Data from this work. [e] Data from ref 33. [f] Data from ref 34.

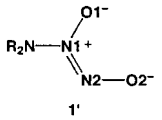

1′

A determination of whether the decomposition proceeds in a concerted one-step fashion through a transient nitric oxide dimer, or by stepwise loss of NO, is not possible with our present data. We have seen no spectral evidence of a transient reduced nitrosamine species that might result from loss of a single NO, although identification of such a reactive intermediate is not likely in the relatively slow time frame of our measurements.

The relative similarity in the kinetically determined pK_{AH} values for **2**−**6**, shown in Table 8, suggests that protonation of the corresponding parent amine nitrogen (as in tautomer A of Scheme 2) is involved in triggering the release of NO from all of these substrates at physiological pH. If this is indeed the case, then the site of the protonation responsible for the spectral shift on lowering the pH (reflected in a pK_a value that is consistently lower by ≥0.5 units than pK_{AH} for all compounds **2**−**6**; see Table 8) must therefore reside in the $[N(O)NO]^-$ group itself. The data in Table 9 would appear to rule out tautomer D as a significant player because N2-methylation or -protonation would be expected to increase λ_{max} (cf. $Me[N(O)NO]^-$), in contrast to the decrease that we found. Transfer of the second proton to tautomer A, resulting in the enhanced rate of NO release at the lower pK_a, must therefore occur at O1 or O2. Protonation at either oxygen would equally well explain the shift in ultraviolet absorbance maximum from 254 to 230 nm that was observed when the pH was lowered from 4 to 2. However, protonation at O1 would yield an ion that can be formally regarded as an *N*-nitroso compound; thus one might expect the observed 254-

(20) Taylor, D. K.; Bytheway, I.; Barton, D. H. R.; Bayse, C. A.; Hall, M. B. *J. Org. Chem.* **1995**, *60*, 435−444.

(21) Keefer, L. K.; Flippen-Anderson, J. L.; George, C.; Shanklin, A. P.; Dunams, T. M.; Christodoulou, D.; Saavedra, J. E.; Sagan, E. S. B. D. S.; Bohle, D. S. Submitted in 2000.

Scheme 2. Possible Monoprotonation Products of **1**

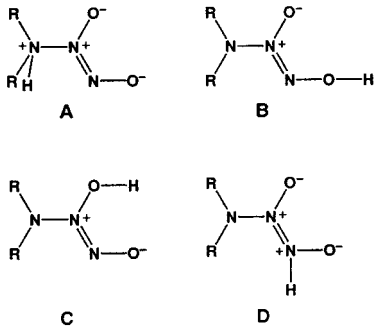

to 230-nm shift to be accompanied by appearance of the n → π^* peak between ~330 and ~400 nm that normally characterizes such structures[22] [including MeN(OMe)−N═O, Table 9]. Increases in absorbance at 340−360 nm were seen on acidifying 10 mM solutions of **6**, but these were too slow to be attributable to proton transfer; we assume that these slow increases in absorbance reflect formation of $R_2N-N{=}O$ species on recombination of autoxidized NO with the secondary amine coproduct of NO release,[7] rather than protonation of tautomer A.

Theoretical calculations of Taylor et al.[20] have shown the charge densities on the O(1) and O(2) oxygens in anions $X[N(O)NO]^-$ to be virtually the same, suggesting that either oxygen would be susceptible to protonation. A comparison of the energies for the optimized geometries of the tautomeric structures X[N(O)NO]H, generated on protonation of the two oxygen sites, however, was reported to show a clear preference for the geometry having the $[N(O)NO]^-$ group protonated at the terminal O2 site, except when strong electron withdrawing groups are present (a situation that exists for **6** when the R_2N nitrogen has already been protonated). With electron density partially delocalized over the diazeniumdiolate group, and with proton shifts between sites being facile and subject to minor polarizations within the $[N(O)NO]^-$ group, a distinction between protonation at O1, O2, or O1 and O2 (i.e., bridging or rapidly equilibrating O-protonation sites) cannot be made with confidence on the basis of the currently available data.

Conclusion

Detailed kinetic studies have shown that diazeniumdiolates release NO with reaction rates that vary, often dramatically, with both pH and structure. Dual protonation states and reaction pathways have been identified for the zwitterionic polyamine substrate **6**. Protonation of the secondary amine nitrogen would appear to be the event responsible for initiating dissociation of NO for compounds **2**−**6** and other diazeniumdiolate substrates at physiological pH.

From comparison of the present data with those for the diazeniumdiolates $K[O_3SN(O)NO]K$[23] and $Na[ON(O)NO]Na$,[24] whose acid-catalyzed decompositions have been shown to yield N_2O rather than NO as their principal gaseous product, it is apparent that the decomposition mechanism adopted is also a sensitive function of the heteroatom to which the diazeniumdiolate functional group is attached.

For amine-derived diazeniumdiolates $R_2N[N(O)NO]^-$, electronic and geometric constraints imposed by R appear to have competing influences on the decomposition of the diazeniumdiolate functional group as well. Such effects must be largely responsible for the remarkable sensitivity to parent amine structure and the wide range of NO dissociation rates that diazeniumdiolate substrates display. For **5** in particular, the surprising degree of dependence on concentration of substrate as well as of certain metal ions may help to explain the reported variability in this zwitterion's half-life from one medium to another.[10,25]

Experimental Section

Compound **2** was synthesized as previously described,[9,26] as were **3**,[27] **4**,[28] **4a**,[29] **5**,[27] **6**,[27] and MeN(OMe)NO.[30]

Kinetic Studies. Rate constants were measured spectrophotometrically by monitoring the decrease in absorbance of the diazeniumdiolate chromophore with Hewlett-Packard 8451 and 8452A Diode Array UV−visible spectrophotometers. In a typical experiment, reaction was initiated by adding a 10-μL aliquot of a stock solution (ca. 10 mM in 10 mM NaOH) to 1.0 mL of buffer in a thermostated UV cell or, for runs with short half-lives requiring rapid mixing, by delivering 1.0-mL aliquots of the buffer, previously thermostated at 37 °C, into 10 μL of the basic diazeniumdiolate stock solution in the cell. With a microprocessor-controlled diode array spectrophotometer, the latter technique enabled the first data points to be collected within ca. 3 s of mixing. Absorbance-time ($A - t$) data obtained from the HP 8451 spectrophotometer were imported into a spreadsheet and first-order rate constants were calculated from a linear regression of the $\ln(A_t - A_\infty)$ plots, which generally showed excellent linearity ($R^2 = 0.999$) over at least 3 half-lives. For measurements involving **5** at 1 mM concentration levels, 100-μL aliquots of reaction mixtures, thermostated at 37 °C, were taken at timed intervals and diluted 10-fold with buffer prior to absorbance measurement. When absorbance changes were examined repetitively over the wavelength range 200−400 nm, isosbestic points were maintained for the duration of the reactions. Data were collected at 37 °C except where indicated otherwise.

No differences were noted in rate constants obtained for **2**−**6** with the HP 8451 and HP 8452A spectrophotometers, despite the more extensive sample irradiation with the former instrument. This speaks against any photochemically induced dissociation pathways with **2**−**6**, although enhanced light-assisted decomposition has been noted with other diazeniumdiolate substrates.[31]

Buffers of 0.10 M phosphate were prepared by weight from $Na_2HPO_4{\cdot}7H_2O$ and $NaH_2PO_4{\cdot}H_2O$, while 0.10 M acetic acid/sodium acetate and 0.050 M glycine/HCl buffers were prepared by partial neutralization of the acid or base with NaOH and HCl, respectively. Tris buffers (0.050 M) were prepared from Tris base and Tris hydrochloride. In all cases, the pH of reaction mixtures was checked by using a JENCO Electronics Microcomputer pH-Vision 6071 pH meter.

UV Spectral Analysis. Measurement of spectral shifts resulting from protonation of the diazeniumdiolate functional group was carried out by adding 10 μL of a freshly prepared 10 mM solution of diazenium-

(22) Lijinsky, W. *Chemistry and Biology of N-Nitroso Compounds*; Cambridge University Press: Cambridge, 1992; pp 60−64.
(23) Switkes, E. G.; Dasch, G. A.; Ackermann, M. N. *Inorg. Chem.* **1973**, *12*, 1120−1123.
(24) Bonner, F. T.; Ravid, B. *Inorg. Chem.* **1975**, *14*, 558−563.
(25) Gow, A. J.; Thom, S. R.; Brass, C.; Ischiropoulos, H. *Microchem. J.* **1997**, *56*, 146−154.
(26) Drago, R. S.; Karstetter, B. R. *J. Am. Chem. Soc.* **1961**, *83*, 1819−1822.
(27) Hrabie, J. A.; Klose, J. R.; Wink, D. A.; Keefer, L. K. *J. Org. Chem.* **1993**, *58*, 1472−1476.
(28) Hrabie, J. A.; Saavedra, J. E.; Davies, K. M.; Keefer, L. K. *Org. Prep. Proced. Int.* **1999**, *31*, 189−192.
(29) Saavedra, J. E.; Booth, M. N.; Hrabie, J. A.; Davies, K. M.; Keefer, L. K. *J. Org. Chem.* **1999**, *64*, 5124−5131.
(30) Boese, A. B., Jr.; Jones, L. W.; Major, R. T. *J. Am. Chem. Soc.* **1931**, *53*, 3530−3541.
(31) Srinivasan, A.; Kebede, N.; Saavedra, J. E.; Nikolaitchik, A. V.; Brady, D. A.; Yourd, E.; Davies, K. M.; Keefer, L. K.; Toscano, J. P. *J. Am. Chem, Soc.* **2001**, *123*, 5465−5472.
(32) Saavedra, J. E.; Srinivasan, A.; Bonifant, C. L.; Chu, J.; Shanklin, A. P.; Flippen-Anderson, J. L.; Rice, W. G.; Turpin, J. A.; Davies, K. M.; Keefer, L. K. Submitted in 2000.
(33) Gowenlock, B. G.; Trotman, J. *J. Chem. Soc.* **1956**, 1670−1675.
(34) Zyuzin, I. N.; Lempert, D. B. *Bull. Acad. Sci. USSR, Div. Chem. Sci. (Engl. Transl.)* **1985**, 753−756.

diolate in 10 mM NaOH to 1.0 mL of buffer in a spectrophotometric cell, and recording the wavelength maximum of the resulting solution appearing between 200 and 300 nm. This was typically obtained within ca. 5 s of mixing before significant decomposition of the substrate has occurred. With the more rapidly reacting diazeniumdiolates, **2** and **3**, the diazeniumdiolate and buffer solutions were cooled to 10 °C prior to mixing. With **5**, measurements were made at both 37 and 10 °C for comparison. NaH_2PO_4/Na_2HPO_4 (pH 8.5−5.4), acetic acid/sodium acetate (pH 5.2−3.6), glycine/HCl (pH 3.6−2.2), 0.01 mM HC1 (pH 2.1), and 0.1 M H_3PO_4 (pH 1.7) were employed as buffers.

Acknowledgment. We thank Dr. J. A. Hrabie for supplying samples of Compounds **3**−**6**. Research was supported in part through National Cancer Institute contract NO1-CO-56000.

Supporting Information Available: Plots of rate data versus $[Fe^{3+}]$ for **5** and versus $[H^+]$ or pH for **2**, **3**, **4**, and **6** (PDF). This material is available free of charge via the Internet at http://pubs.acs.org.

JA002899Q